

ORIGINAL ARTICLE

Mycophenolate mofetil attenuates liver ischemia/reperfusion injury in rats

Yuan-Xing Liu,^{1,2} Li-Ming Jin,^{1,2} Lin Zhou,^{1,2} Hai-Yang Xie,^{1,2} Guo-Ping Jiang,^{1,2} Yan Wang,^{1,2} Xiao-Wen Feng,^{1,2} Hui Chen,^{1,2} Sheng Yan³ and Shu-Sen Zheng^{1,2,3}

1 Key Laboratory of Combined Multi-organ Transplantation, Ministry of Public Health, Hangzhou, Zhejiang Province, China

2 Key Laboratory of organ Transplantation, Zhejiang Province, China

3 Division of Hepatobiliary and Pancreatic Surgery, Department of Surgery, First Affiliated Hospital, School of Medicine, Zhejiang University, Hangzhou, Zhejiang Province, China

Keywords

ischemia/reperfusion injury, microcirculation, mitogen-activated protein kinases, mycophenolate mofetil, reactive oxygen species.

Correspondence

Shu-Sen Zheng MD, PhD, Department of Hepatobiliary Pancreatic Surgery, Key Laboratory of Combined Multiorgan Transplantation, Ministry of Public Health, First Affiliated Hospital of Medical College, Zhejiang University, Hangzhou 310003, China. Tel.: 86 571 87236601; fax: 86 571 87236884; e-mail: shusenzheng@zju.edu.cn

Received: 1 December 2008

Revision requested: 29 December 2008

Accepted: 22 February 2009

doi:10.1111/j.1432-2277.2009.00866.x

Summary

Mycophenolate mofetil (MMF) has been gradually introduced into clinical liver transplantation in recent years. However, the effects of MMF on hepatic ischemia/reperfusion (I/R) injury and the potential mechanisms involved are not totally understood. We aimed to evaluate whether MMF could attenuate hepatic I/R injury. MMF (20 mg/kg) or vehicle was administered to Wistar rats by gavage. The rats were then subjected to hepatic ischemia. Liver cell apoptosis and the levels of aspartate aminotransferase, myeloperoxidase (MPO), xanthine oxidase (XOD) and malondialdehyde (MDA) were determined. Expression of vascular cell adhesion molecule-1 (VCAM-1) and activation of mitogen-activated protein kinases (MAPKs) were also investigated. Furthermore, the hepatic microcirculation was observed by intravital fluorescence microscopy. Rats pretreated with MMF exhibited significant alleviation of their postschemic liver function. Liver cell apoptosis and the tissue MPO, XOD and MDA levels were decreased by MMF pretreatment. MMF also improved I/R-induced hemodynamic turbulence, as evidenced by reduced hepatic perfusion failure and decreased numbers of rolling and adherent leukocytes. I/R injury induced activation of the MAPKs pathway while expression of VCAM-1 was downregulated by MMF pretreatment. In summary, MMF attenuates hepatic I/R injury through suppression of the production of reactive oxygen species and amelioration of postschemic microcirculatory disturbances.

Introduction

Hepatic ischemia/reperfusion (I/R) injury is one of the most common causes of early allograft dysfunction in liver transplanted patients and represents an additional risk factor for long-term survival after transplantation [1]. The destructive effects of I/R injury are the result of a complex pathophysiological process with a number of contributory factors. Previous investigations have shown that overproduction of reactive oxygen species (ROS) and hepatic microcirculation disturbances, which are characterized by capillary perfusion failure and increased leukocyte adherence, are important aspects of hepatic I/R

injury [2–4]. By targeting these aspects, the development of pharmaceutical strategies to attenuate hepatic I/R injury is important for achieving better clinical outcomes.

Previous evidence has indicated that immunosuppressive drugs, which are inevitably used in transplantation, have impacts on organ I/R injury [5–7]. Mycophenolate mofetil (MMF), the morpholinoethyl ester of mycophenolic acid (MPA), is a powerful immunosuppressant that is currently used for the prevention of acute organ graft rejection [8]. *In vivo*, MMF is rapidly de-esterified to MPA and further metabolized to the glucuronidated metabolite MPA glucuronide. MPA depletes guanosine triphosphate pools in lymphocytes and monocytes and

suppresses *de novo* synthesis of purines, thereby exerting selective and reversible antiproliferative effects on these cells [9]. Previous studies have demonstrated that purine metabolites produced during ischemia can contribute to the production of harmful free radicals via xanthine oxidase (XOD), and that inhibition of XOD prevents postischemic ROS generation and hepatic injury [10–12]. Data obtained from a cardiomyocytes enriched model revealed that MMF can reduce the postischemic increases in xanthine and hypoxanthine, and subsequently alleviate the generation of free radical species [13]. In addition, guanosine depletion can inhibit the transfer of mannose and fucose residues to glycoproteins, including cell adhesion molecules. Earlier experimental studies on human monocytes and renal ischemia in rats have suggested MMF can inhibit the overexpression of ICAM-1 and suppress leukocyte–endothelial cell interactions, which play central roles in I/R injury [14–16].

In recent years, MMF has been gradually introduced into clinical liver transplantation as an immunosuppressive drug [17–19]. As transplanted livers are subject to I/R injury, the potential effects of MMF on the process of hepatic I/R injury are of considerable importance. However, the impact of MMF on hepatic I/R injury remains unclear.

Materials and methods

Animal procedures

Male Wistar rats ($n = 216$; body weight, 230–250 g) were purchased from Shanghai Animal Center (Chinese Academy of Science, Shanghai, China). The animals were housed under standard animal care conditions and fed with rat chow *ad libitum*. All animal experiments were approved by the Animal Care Committee of Zhejiang University in accordance with the Principles of Laboratory Animal Care (NIH publication 85-23, revised 1985).

The rats were assigned into four groups. Group 1 (IR+M) underwent the hepatic I/R procedure and received 20 mg/kg of MMF (Cellcept[®]; Roche Pharmaceuticals, Basingstoke, UK) in the drug vehicle (0.5% sodium carboxymethylcellulose). Group 2 (IR+V) underwent the same procedure and received the vehicle alone. Group 3 (M) underwent a sham operation and received MMF on the same schedule. Group 4 (C) underwent a sham operation and received the vehicle alone. All treatments were administered daily by gavage from 5 days prior to ischemia until the animals were killed.

All surgical procedures were performed under general anesthesia using sodium pentobarbital (60 mg/kg *i.p.*). After a midline laparotomy was performed, 70% hepatic ischemia was induced by clamping the portal vein, hepatic artery and bile duct supplying the median and left

lobes of the liver with a microvascular clip [20]. As the blood supply to the omental and right lobes remained uninterrupted, intestinal congestion was avoided during clamping by the bypass portal flow through the nonischemic lobes. The duration time of the partial hepatic ischemia was chosen on the basis of a pilot experiment, in which 60 min of ischemia caused pronounced liver injury without any fatal accidents such as severe liver failure or death of the animals. After 60 min of partial hepatic ischemia, the clip was removed to initiate hepatic reperfusion and the abdominal cavity was closed with a 4-0 silk suture. The animals were allowed to recover from the anesthesia and given free access to food and water. Sham-operated groups underwent the same procedures without clamping the pedicle of the liver lobes.

The animals were then assigned to the four experimental groups, according to the phase of the study and the treatment.

Phase one

This phase was undertaken in 192 rats assigned to the four experimental groups. The animals were killed after reperfusion at eight sampling time points (0.5, 1, 2, 4, 12 h, 1, 2 or 4 days) ($n = 6$ per time point). A blood sample collected from the inferior vena cava of each rat at kill was centrifuged, and the serum was stored at $-80\text{ }^{\circ}\text{C}$ until analysis. Liver tissue samples (3-mm cubes) were removed from each rat. Some of these samples were snap-frozen in isopentane precooled with liquid nitrogen at $-155\text{ }^{\circ}\text{C}$ and stored at $-80\text{ }^{\circ}\text{C}$, while other samples were fixed in 4% (v/v) paraformaldehyde and stored at $4\text{ }^{\circ}\text{C}$. Serum aspartate aminotransferase (AST), which is regarded to show the best correlation with the degree of hepatic I/R injury [21,22], was determined to identify the moment at which the greatest liver damage occurred.

Phase two

The rate of apoptosis and levels of myeloperoxidase (MPO), XOD and malondialdehyde (MDA), as well as the gene and protein expression levels of vascular cell adhesion molecule-1 (VCAM-1), were evaluated with the samples obtained in phase one at the experimental moment associated with the most dramatic morphologic changes based on the phase one experiments, namely 4 h.

Phase three

A separate set of 24 rats was set aside for intravital fluorescence microscopy analysis and divided into the four experimental groups ($n = 6$ per group). After 60–120 min of reperfusion, these rats were anesthetized again and subjected to intravital fluorescence microscopy studies. Subsequently, all these animals were killed without any blood or tissue samples being taken.

Biochemical determinations

AST assay

To assess liver damage, hepatic injury was evaluated by determination of the AST levels using an Automated Chemical Analyzer (7600; Hitachi, Tokyo, Japan).

Myeloperoxidase, XOD and MDA assays

For assessment of neutrophil sequestration and activation in the ischemic liver, the MPO contents were measured. Postischemic liver XOD activities in the liver tissues were also evaluated. Lipid peroxidation, an indicator of oxidative injury, was determined by measuring the formation of MDA. The liver tissue MPO, XOD and MDA levels were assayed using commercial kits (NJJC Bio Inc., Nanjing, China), according to the manufacturer's instructions.

Terminal transferase-mediated dUTP nick end-labeling staining

Paraffin-embedded sections were prepared and stained for apoptotic cells by the terminal transferase-mediated dUTP nick end-labeling (TUNEL) method using a commercially available kit (Apop Tag Peroxidase *In Situ* Apoptosis Detection Kit S7100; Chemicon International Inc., Billerica, MA, USA). The TUNEL assay was performed according to the manufacturer's protocol. The results were presented as the mean number of TUNEL-positive cells per high power field [23].

Western blot analysis

The protein expression levels of VCAM-1 and mitogen-activated protein kinases (MAPKs), namely extracellular signal-regulated kinase 1/2 (ERK1/2), c-Jun NH₂-terminal kinase (JNK) and p38 MAPK, were evaluated by western blotting. Protein samples (50 µg) were denatured in reducing buffer and separated by SDS-PAGE using a 10% polyacrylamide gel. The separated proteins were transferred to polyvinylidene difluoride membranes. After blocking with 5% nonfat dry milk in TBS-0.1% Tween-20 for 1 h at room temperature, the membranes were incubated with primary antibodies against VCAM-1 (Santa Cruz Biotechnology Inc., Santa Cruz, CA, USA) and the phosphorylated and total forms of ERK1/2, JNK and p38 (Cell Signaling, Beverly, MA, USA) at a dilution of 1:1000 in TBS-0.1% Tween overnight at 4 °C. The membranes were then incubated with a secondary antibody, peroxidase-conjugated goat anti-rabbit immunoglobulin G, at a dilution of 1:2000 for 1 h at room temperature. After washing, the membranes were analyzed using an enhanced chemiluminescence system (EZ-ECL; Beit

Haemek Ltd, Ashrat, Israel) according to the manufacturer's protocol.

Real-time polymerase chain reaction

Gene expression of VCAM-1 was assessed by quantitative real-time polymerase chain reaction (PCR). Total RNA was extracted from frozen liver samples with the TRIzol Reagent (Invitrogen Corporation, Carlsbad, CA, USA), and 1 µg of RNA from each sample was reverse-transcribed with oligo (dT) and random hexamer primers using M-MLV reverse transcriptase (Promega Corporation, Madison, WI, USA). Next, 10 ng of cDNA and gene-specific primers were added to SYBR Green PCR Master Mix (SYBR Green I Dye, AmpliTaq DNA polymerase, dNTPs with dUTP and optimal buffer components; Applied Biosystems, Foster City, CA, USA) and subjected to PCR amplification in an iCycler Real-Time PCR Detection System (Bio-Rad, Hercules, CA, USA). Fluorescence was measured after each PCR cycle (initial 10-min denaturation at 95 °C, followed by 40 amplification cycles of denaturation at 95 °C for 15 s and annealing extension at 61 °C for 1 min). Each sample was measured in triplicate and the VCAM-1 gene expression was normalized by the endogenous glyceraldehyde-3-phosphate dehydrogenase (GAPDH) gene expression. Relative quantifications of target genes were standardized by the sham-operated samples using the comparative *C*(t) method using threshold cycle *C*(t) values. The sequences of the primers used were: 5'-GAAGCCGGTCATGGTCAAGT-3' and 5'-GACGGTCACCCTTGAACAGTC-3' for VCAM-1 (cDNA: NM_012889); and 5'-ATGCCATCACTGCCACTCAG-3' and 5'-CAGGGATGATGTTCTGGGT-3' for GAPDH (cDNA: DQ_403053).

Intravital fluorescence microscopy

Liver microcirculation was assessed during the time period of 60–120 min after reperfusion by intravital fluorescence microscopy using a previously described method [24] with some modifications. The rat was placed in a prone position, and the left liver lobe was placed on a immersion glass disc in warm saline at 37 °C. Intravital fluorescence microscopy was performed using a modified Olympus microscope (IX81WI; Olympus Optical Corporation GmbH, Hamburg, Germany). Blood perfusion was evaluated after contrast enhancement with fluorescein-isothiocyanate-labeled dextran (FITC-dextran; i.v. 0.4 ml, 4 mg/ml; Sigma Chemical Co., St. Louis, MO, USA). Leukocytes were labeled *in vivo* with rhodamine-6G (i.v. 0.1 ml, 4 mg/ml; Sigma Chemical Co.). Ten postsinusoidal venules with connecting sinusoids were evaluated in each animal (*n* = 6 per group).

Filter blocks for FITC-dextran (excitation: 450–480 nm; emission: >515 nm) and rhodamine 6G (excitation: 510–550 nm; emission: >590 nm) were used for epi-illumination. An objective (UPlanFLN 20 × 0.45 Ph1; Olympus Optical Corporation GmbH) provided a magnification of approximately 320 on the video screen. Observations were recorded using a charge-coupled device video camera (DP30BW CCD camera; Olympus Optical Corporation GmbH) and stored. The video images were analyzed using Image Pro plus 6.0 (Media Cybernetics Inc., Bethesda, MD, USA).

The quantitative analyses of liver microcirculation included the determination of the number of perfused sinusoids, given as a percentage of the total number of sinusoids. Rolling leukocytes were defined as cells that were loosely interacting with the venular endothelium and could easily be discriminated by their visibly slower flow rate. Adherent leukocytes were defined as cells that remained attached to the same area of endothelial lining for the entire 30-s observation period. The observed numbers of rolling and adherent leukocytes in 10 randomly selected postcapillary venules were expressed as cells/min and cells/mm venule length, respectively. Sinusoidal trapping was measured by counting the number of cells that adhered in liver sinusoids in 10 high power fields and given as cells/high power field.

Statistical analysis

All values are reported as the mean ± SD. Data were analyzed by one-way ANOVA, and a Student–Newman–Keuls posttest was used for estimation of the stochastic probability in intergroup comparisons. Values of $P < 0.05$ were considered to indicate statistical significance.

Results

Analysis of liver function by AST determination

As shown in Fig. 1, significant increases in the serum AST activities were observed after I/R from 0.5 h to 2 days in the IR+V group compared with the C group, indicating impaired liver function after I/R injury. In contrast, the postschemic serum AST activities were significantly lower in the IR+M group. These results showed that administration of MMF can effectively ameliorate the impairment of liver function after I/R injury. There was no significant difference between the serum AST levels in the M and C groups, indicating that MMF had no influence on nonischemic liver function (Fig. 1).

Tissue MPO, XOD and MDA levels

There were no differences in the tissue MPO, XOD and MDA levels between vehicle- and MMF-treated rats in

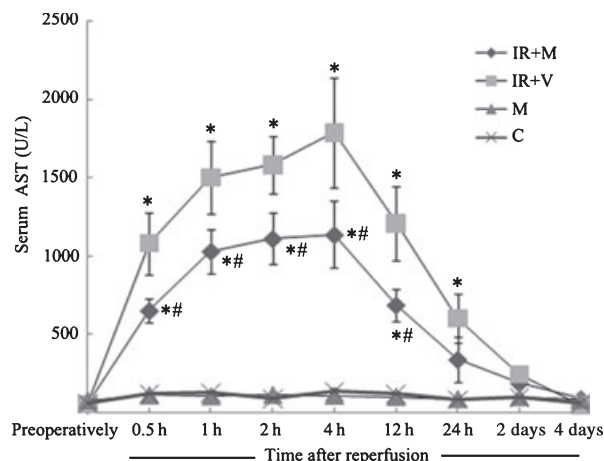


Figure 1 Serum AST levels in each group at specified time points after surgery. Compared with the C group, both the IR+V and IR+M groups show significant increases in their serum AST levels ($P < 0.05$), which peak at 4 h and then return to similar levels to those in the nonischemia groups after 2 days. In the IR+M group, liver function is preserved compared with the IR+V group ($P < 0.05$). Administration of MMF in nonischemic livers has no influence on the serum AST activities (M group versus C group, $P > 0.05$). Values are means ± SD. * $P < 0.05$ versus C group; # $P < 0.05$ versus IR+V group.

the sham-operated groups (C group versus M group, $P > 0.05$, data not shown). Hepatic I/R injury led to elevation of the tissue MPO, XOD and MDA levels at 4 h after reperfusion (IR+V group versus C group and IR+M group versus C group, $P < 0.05$), and the increases in the MPO, XOD and MDA levels were significantly inhibited by treatment with MMF (IR+M group versus IR+V group, $P < 0.05$) (Table 1).

TUNEL staining

No apoptotic cells were detected in nonischemic livers. The number of TUNEL-positive cells was 8.2 ± 1.4 cells/high

Table 1. Tissue levels of MPO, XOD and MDA.

	C group	IR+V group	IR+M group
MPO (U/g wet tissue)	1.53 ± 0.31	3.96 ± 0.42*	3.02 ± 0.35*†
XOD (U/g protein)	4.21 ± 0.53	12.36 ± 2.77*	9.08 ± 1.64*†
MDA (nmol/mg protein)	2.31 ± 0.25	4.89 ± 0.68*	3.35 ± 0.29*†

After 4 h of reperfusion, the livers were harvested, and the tissue levels of MPO, XOD and MDA were assessed. Administration of MMF significantly decreases the I/R injury-induced elevation of the MPO, XOD and MDA levels.

Data are shown as the mean ± SD ($n = 6$ for each group).

* $P < 0.05$, versus C group.

† $P < 0.05$, versus IR+V group.

power field in the IR+V group, compared with only 1.9 ± 0.3 TUNEL-positive cells/high power field in the IR+M group (IR+M group versus IR+V group, $P < 0.05$) (Fig. 2).

VCAM-1 mRNA and protein expression levels

As shown in Fig. 3a, VCAM-1 protein expression was enhanced in both IR+V and IR+M groups compared with the sham-operated group at 4 h after I/R injury. In contrast, MMF significantly decreased the hepatic VCAM-1 protein level (Fig. 3a).

VCAM-1 mRNA expression was determined by real-time PCR. The results were almost the same as those obtained in the western blot analyses. As shown in Fig. 3e, liver I/R injury significantly upregulated VCAM-1 mRNA expression compared with the sham-operated group, whereas MMF treatment significantly decreased I/R-induced VCAM-1 mRNA expression (Fig. 3e).

Expression of MAPK proteins

Compared with the sham-operated group, hepatic I/R injury markedly increased the phosphorylation of ERK, p38 MAPK and JNK in the IR+V group. In the IR+M group, the protein expressions of phospho-ERK and phospho-p38 MAPK were downregulated. Phospho-JNK was not influenced by MMF treatment. The total amounts of ERK1/2, p38 MAPK and JNK remained unchanged in all groups (Fig. 3b–d).

Sinusoidal perfusion rate

Analysis of the hepatic microcirculation by intravital fluorescence microscopy revealed marked perfusion failure after I/R injury compared with sham-operated animals, as indicated by the increased number of nonperfused sinusoids. The perfused sinusoid rates were much lower in the IR+V ($65.6 \pm 3.6\%$) and IR+M ($78.2 \pm 11.5\%$) groups than in the C ($97.1 \pm 2.1\%$) group. Although the difference between the IR+V and IR+M groups did not reach

statistical significance ($P > 0.05$), MMF pretreatment showed better sinusoidal perfusion than the vehicle group (Table 2).

Leukocyte–endothelial cell interactions

Only a few sequestered leukocytes were found in the postsinusoidal venules of sham-operated animals. The numbers of rolling and adherent leukocytes in postsinusoidal venules were 1.1 ± 0.3 and 0.3 ± 0.1 cells/mm venule length, respectively. Sinusoidal leukocyte adhesion assessments elicited similar results to the low sinusoidal trapping (0.4 ± 0.1 cells/high power field) in sham-operated animals. Hepatic I/R injury provoked activation of leukocytes, as indicated by their enhanced interactions with the venular endothelium within the hepatic microvasculature. The numbers of rolling and adherent leukocytes in postsinusoidal venules (32.6 ± 6.1 and 21.7 ± 5.2 cells/mm venule length, respectively) were more pronounced in the IR+V group than in the C group. In sinusoids, I/R injury increased sinusoidal trapping to 22.4 ± 4.2 cells/high power field. Notably, pretreatment with MMF significantly decreased the leukocyte–endothelium interactions in the liver, with nearly threefold decreases in the numbers of rolling and adherent leukocytes in the IR+M group (11.8 ± 2.7 and 7.6 ± 0.9 cells/mm venule length, respectively). MMF administration was also characterized by reduced sequestration of leukocytes in the sinusoids with lower sinusoidal trapping (4.6 ± 0.8 cells/high power field) compared with the IR+V group (Table 2, Fig. 4).

Discussion

The present study has demonstrated that administration of MMF confers protection against hepatic I/R injury, as evidenced by significant amelioration of liver function and liver cell apoptosis during hepatic I/R. These protective effects appear to be associated with reduced inflammatory responses and production of ROS, together with improvement in I/R-induced hemodynamic turbulence.

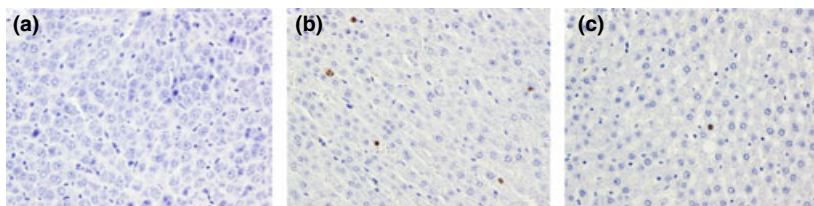


Figure 2 Detection of apoptotic cells using the TUNEL method. No TUNEL staining is observed in a section from the C group (a). After 60 min of ischemia and 4 h of reperfusion, a section from the IR+V group shows a large number of TUNEL-positive cells (b), whereas the proportion of TUNEL-positive cells is significantly lower in a section from the IR+M group (c).

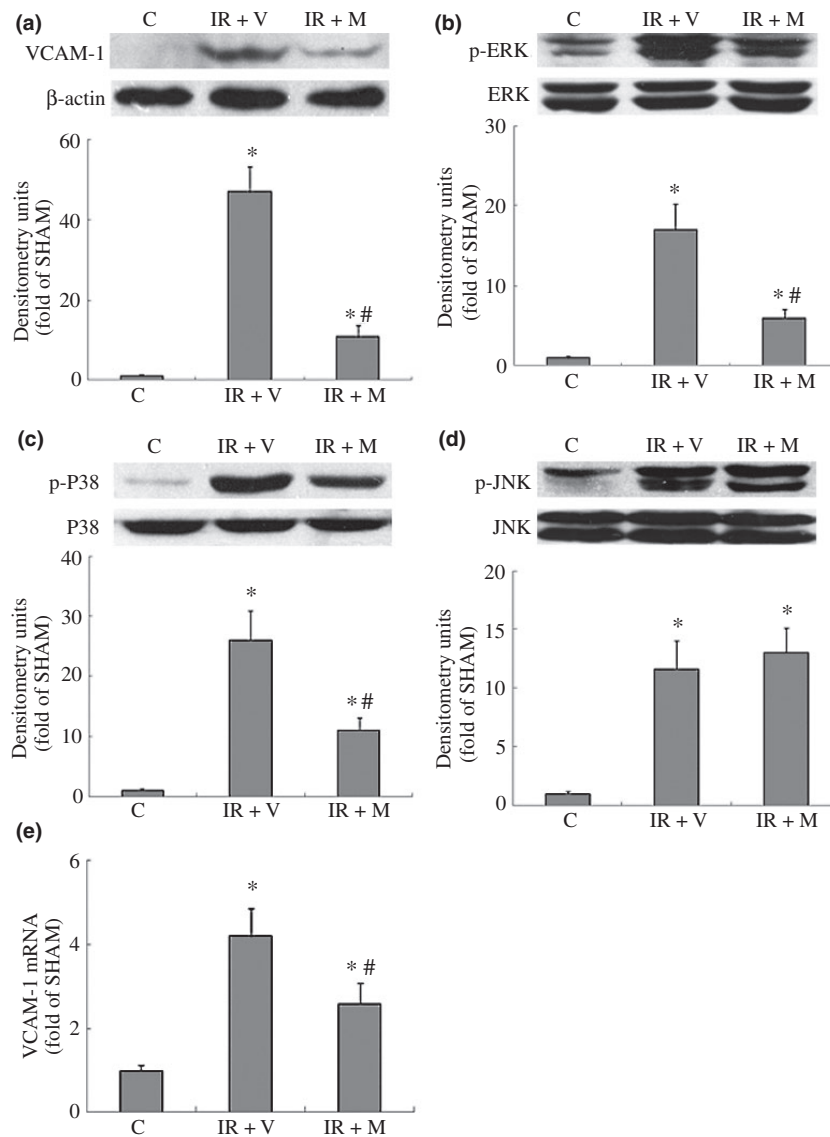


Figure 3 Effects of MMF on VCAM-1 expression and MAPKs phosphorylation in liver I/R injury. Representative western blot (upper panel) and densitometric (lower panel) analyses are presented to show the influence of MMF on VCAM-1 expression and ERK 1/2, p38 MAPK and JNK activation in the livers of the different groups. (a) Effects of MMF on I/R injury-induced VCAM-1 expression. (b) Effects of MMF on I/R injury-induced ERK1/2 activation. (c) Effects of MMF on I/R injury-induced p38 MAPK activation. (d) Effects of MMF on I/R injury-induced JNK activation. (e) Effects of MMF on VCAM-1 mRNA expression in livers evaluated by real-time PCR analysis. The VCAM-1 mRNA level was corrected by the corresponding GAPDH mRNA level in each sample. Bars represent the fold increases compared with the sham-operated group. Each value represents the mean \pm SD of three experiments. * $P < 0.05$, versus C group; # $P < 0.05$, versus IR+V group.

ROS and toxic free radicals have been implicated in the mediation of hepatic I/R injury [25–27]. In this study, MMF treatment markedly reduced tissue MPO levels, indicating suppression of neutrophil sequestration and activation, which play fundamental roles in I/R-induced ROS production [28,29]. Another mechanism for the important beneficial effects of MMF on ROS abatement is nucleotide metabolism. The influence of MMF on nucleotide metabolism is not only its major immunosuppressive mechanism but also involved in its antioxidative effects [13,30–32]. The metabolism of xanthine and hypoxanthine was shown to play a part in I/R-induced ROS generation. During the period of ischemic injury, adenosine triphosphate is degraded to adenosine monophosphate and subsequently catabolized to hypoxanthine. Upon reperfusion of the ischemic tissue, hypoxanthine serves as a

substrate for XOD with subsequent production of tissue-damaging superoxide radicals [33]. Previous studies have demonstrated that XOD activation contributes to the development of hepatic I/R. Inhibition of XOD results in lower postischemic ROS levels and consequently reduces hepatic MDA activity and transaminase levels [2,11]. Previous data from a cardiomyocyte-enriched model revealed that I/R injury results in significant increases in xanthine and hypoxanthine, and that MMF treatment can display its inosine monophosphate dehydrogenase inhibition potency, as revealed by strong decreases in the production of xanthine and hypoxanthine, and consequent reduction in XOD-dependent free radical production [13]. In this study, MMF treatment significantly decreased

Table 2. Intravital analysis of liver microcirculation.

	C group	IR+V group	IR+M group
Perfused sinusoids rate (%)	97.1 ± 2.1%	65.6 ± 13.6%*	78.2 ± 11.5%*
Rolling leukocytes (cells/min)	1.1 ± 0.3	32.6 ± 6.1*	11.8 ± 2.7*†
Adherent leukocytes (cells/mm venule length)	0.3 ± 0.1	21.7 ± 5.2*	7.6 ± 0.9*†
Sinusoidal trapping (Cell/high power field)	0.4 ± 0.1	22.4 ± 4.2*	4.6 ± 0.8*†

Quantitative analysis of the liver microcirculation was performed by intravital microscopy. The perfused sinusoid rate was expressed as a percentage of the total number of sinusoids. Rolling leukocytes were calculated as the number of cells per minute during the observation period (min^{-1}). Adherent leukocytes were expressed as the number of cells per venule length (mm^{-1}). Sinusoidal trapping was calculated as the number of cells per high power field.

Data are shown as the mean ± SD ($n = 6$ for each group).

* $P < 0.05$, versus C group.

† $P < 0.05$, versus IR+V group.

I/R-induced tissue XOD activation and consequently attenuated oxidative stress-induced hepatic injury, as indicated by the preservation of the tissue MDA levels. To date, the mechanisms for the inhibitory effects of MMF with regard to XOD activity remain unclear. A possible mechanism may be that MMF reduces neutrophil activation, as previous studies have demonstrated important roles of neutrophil accumulation in XOD-mediated reperfusion injury [34,35]. Other mechanisms, such as purine depletion causing substrate reduction, are also worthy of further investigation.

Microcirculatory disturbances during organ transplantation, which are characterized by capillary perfusion failure and inflammation-associated leukocyte recruitment, are thought to be a key step in the cascade of events involved in I/R injury [36]. After I/R injury, microcirculatory disturbances can be initiated by the generation of ROS and other proinflammatory mediators that activate both leukocytes and the hepatic vascular endothelium. Upon activation, leukocytes roll along the endothelium of postsinusoidal venules and subsequently adhere to the endothelium. Amelioration of such posts ischemic leukocyte–endothelial cell interactions can protect the liver against I/R injury [3,37,38]. In this study, analysis of leukocyte–endothelial cell interactions by intravital fluorescence microscopy revealed that the posts ischemic increases in the numbers of rolling and adherent leukocytes were significantly reduced in MMF-pretreated rats. Amelioration of post-I/R sinusoidal perfusion failure was also observed in the MMF-pretreated rats. These observations indicated that MMF has beneficial hemodynamic effects on hepatic I/R by alleviating posts ischemic leukocyte–endothelial cell interactions. The expression of adhesion molecules, such as VCAM-1, is generally required for firm adhesion between leukocytes and the hepatic vascular endothelium [39,40], and downregulation of VCAM-1 can attenuate hepatic I/R injury both *in vivo* and *in vitro* [41,42]. Several studies have shown that VCAM-1 is essential for leukocyte attachment and penetration through endothelial cells in hepatic sinusoids and postsinusoidal venules of the posts ischemic liver [43,44]. In this study, the amelioration of microcirculatory disturbances and reduced leukocyte–endothelial cell interactions

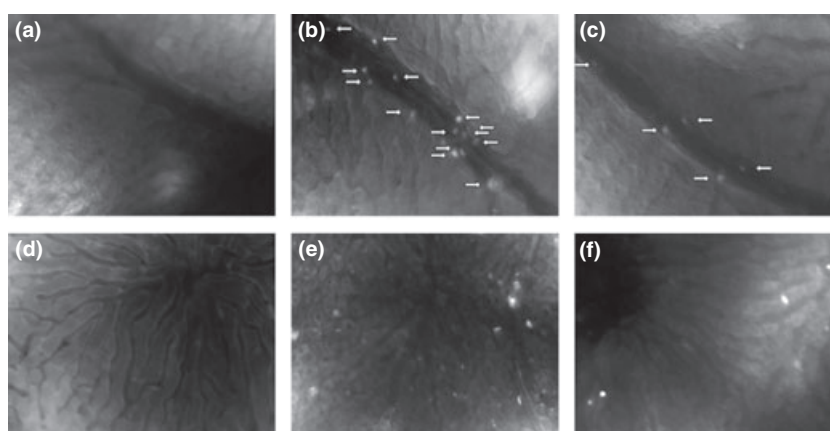


Figure 4 Intravital fluorescence microscopy of hepatic microcirculation using rhodamine 6G in postsinusoidal venules and sinusoids, showing fluorescently labeled rolling and adherent leukocytes as well as sequestration of leukocytes in sinusoids. (a) Rolling and adherent leukocytes in the C group. (b) Rolling and adherent leukocytes in the IR+V group. (c) Rolling and adherent leukocytes in the IR+M group. (d) Sinusoidal sequestration of leukocytes in the C group. (e) Sinusoidal sequestration of leukocytes in the IR+V group. (f) Sinusoidal sequestration of leukocytes in the IR+M group.

achieved by preischemic administration of MMF were associated with decreased tissue VCAM-1 mRNA and protein levels, which were both increased after I/R. These results are consistent with a renal previous study, which found that MPA can suppress leukocyte–endothelial cell interactions by inhibiting the expression of adhesion molecules [15]. A potential mechanism may involve the inhibitory actions of MMF on adhesion molecule synthesis. By depleting guanosine triphosphate pools, MMF inhibits fucose and mannose transfer to membrane glycoproteins, including adhesion molecules [15,32]. Moreover, MAPKs, which are key elements in the regulation of cellular responses to external inflammatory signals during hepatic I/R injury [45,46], may also contribute to the inhibitory effects of MMF on adhesion molecules. Some studies have demonstrated that MAPKs are important for the expression of endothelial adhesion molecules [47–49]. On the other hand, MPA treatment was reported to cause marked downregulation of the p38 MAPK and ERK1/2 pathways in mesangial and myeloid cells [50,51], and exogenous guanosine can rescue the MMF inhibitory effects on MAPKs, thereby indicating that guanosine reduction is partially responsible for the inhibitory effects of MPA on MAPKs activation [50]. In our experiments, hepatic I/R injury increased the phosphorylation of ERK, p38 MAPK and JNK, and administration of MMF markedly downregulated the phospho-ERK and phospho-p38 MAPK levels. Therefore, we conclude that MMF appears to downregulate the postischemia expression levels of adhesion molecules as well as the subsequent leukocyte–endothelial cell interactions, at least partly through guanosine reduction-induced inhibition of ERK and p38 MAPK phosphorylation and activation.

At the present time, our study is simply proof of a concept for clinical liver transplantation in a nonclinical setting, and MMF is only used in recipients. Under such circumstances, MMF can only show its effects during the phase of reperfusion. Therefore, administration of MMF at the time point of reperfusion is also worthy of further investigation.

In summary, pretreatment with MMF attenuated hepatic I/R injury in rats in association with both decreased production of ROS and beneficial hemodynamic effects by inhibiting leukocyte–endothelial cell interactions through downregulation of the adhesion molecule VCAM-1. Therefore, MMF used as part of an immunosuppressant regimen may also afford potential protective effects against hepatic ischemia.

Authorship

Y-XL: designed and performed study, collect and analyze data, wrote the paper. L-MJ: performed study and collect

data. LZ: designed study. H-YX, G-PJ, and YW: performed study. X-WF: contributed to the histological examinations. HC: performed the animal surgery. SY: contributed important reagents. S-SZ: designed and conducted the research.

Funding sources

None.

Acknowledgements

This study was supported by the National Basic Research Program of China (973 Program) (No. 2009cb522403) and the Major Program of the Science and Technology Bureau of Zhejiang Province, China (No. 2006C13020).

References

1. Totsuka E, Fung U, Hakamada K, *et al.* Analysis of clinical variables of donors and recipients with respect to short-term graft outcome in human liver transplantation. *Transplant Proc* 2004; **36**: 2215.
2. Fernandez L, Heredia N, Grande L, *et al.* Preconditioning protects liver and lung damage in rat liver transplantation: role of xanthine/xanthine oxidase. *Hepatology* 2002; **36**: 562.
3. El-Badry AM, Moritz W, Contaldo C, Tian Y, Graf R, Clavien PA. Prevention of reperfusion injury and microcirculatory failure in macrosteatotic mouse liver by omega-3 fatty acids. *Hepatology* 2007; **45**: 855.
4. Burkhardt M, Slotta JE, Garcia P, Seekamp A, Menger MD, Pohlemann T. The effect of estrogen on hepatic microcirculation after ischemia/reperfusion. *Int J Colorectal Dis* 2008; **23**: 113.
5. Matsuda T, Yamaguchi Y, Matsumura F, *et al.* Immunosuppressants decrease neutrophil chemoattractant and attenuate ischemia/reperfusion injury of the liver in rats. *J Trauma* 1998; **44**: 475.
6. Crenesse D, Laurens M, Heurteaux C, *et al.* Rat liver ischemia-reperfusion-induced apoptosis and necrosis are decreased by FK506 pretreatment. *Eur J Pharmacol* 2003; **473**: 177.
7. Frink M, Kaudel CP, Hildebrand F, *et al.* FTY720 improves survival after transient ischemia and reperfusion of the hind limbs. *J Trauma* 2007; **63**: 263.
8. Halloran P, Mathew T, Tomlanovich S, Groth C, Hooffman L, Barker C. Mycophenolate mofetil in renal allograft recipients: a pooled efficacy analysis of three randomized, double-blind, clinical studies in prevention of rejection. The International Mycophenolate Mofetil Renal Transplant Study Groups. *Transplantation* 1997; **63**: 39.
9. Fraser-Smith EB, Rosete JD, Schatzman RC. Suppression by mycophenolate mofetil of the neointimal thickening

- caused by vascular injury in a rat arterial stenosis model. *J Pharmacol Exp Ther* 1995; **275**: 1204.
10. McCord JM. Oxygen-derived free radicals in postischemic tissue injury. *N Engl J Med* 1985; **312**: 159.
 11. Peralta C, Bulbena O, Xaus C, et al. Ischemic preconditioning: a defense mechanism against the reactive oxygen species generated after hepatic ischemia reperfusion. *Transplantation* 2002; **73**: 1203.
 12. Leon Fernandez OS, Ajamieh HH, Berlanga J, et al. Ozone oxidative preconditioning is mediated by A1 adenosine receptors in a rat model of liver ischemia/ reperfusion. *Transpl Int* 2008; **21**: 39.
 13. Bes S, Tatou E, Vandroux D, Tissier C, Rochette L, Athias P. Physiological and metabolic actions of mycophenolate mofetil on cultured newborn rat cardiomyocytes in normoxia and in simulated ischemia. *Fundam Clin Pharmacol* 2004; **18**: 287.
 14. Laurent AF, Dumont S, Poindron P, Muller CD. Mycophenolic acid suppresses protein N-linked glycosylation in human monocytes and their adhesion to endothelial cells and to some substrates. *Exp Hematol* 1996; **24**: 59.
 15. Ventura CG, Coimbra TM, de Campos SB, de Castro I, Yu L, Seguro AC. Mycophenolate mofetil attenuates renal ischemia/reperfusion injury. *J Am Soc Nephrol* 2002; **13**: 2524.
 16. Olschewski P, Hunold G, Eipel C, et al. Improved microcirculation by low-viscosity histidine- tryptophan-ketoglutarate graft flush and subsequent cold storage in University of Wisconsin solution: results of an orthotopic rat liver transplantation model. *Transpl Int* 2008; **21**: 1175.
 17. Wiesner R, Rabkin J, Klintmalm G, et al. A randomized double-blind comparative study of mycophenolate mofetil and azathioprine in combination with cyclosporine and corticosteroids in primary liver transplant recipients. *Liver Transpl* 2001; **7**: 442.
 18. Fisher RA, Stone JJ, Wolfe LG, et al. Four-year follow-up of a prospective randomized trial of mycophenolate mofetil with cyclosporine microemulsion or tacrolimus following liver transplantation. *Clin Transplant* 2004; **18**: 463.
 19. Ringe B, Braun F, Schutz E, et al. A novel management strategy of steroid-free immunosuppression after liver transplantation: efficacy and safety of tacrolimus and mycophenolate mofetil. *Transplantation* 2001; **71**: 508.
 20. Taniguchi M, Uchinami M, Doi K, et al. Edaravone reduces ischemia-reperfusion injury mediators in rat liver. *J Surg Res* 2007; **137**: 69.
 21. Selzner M, Rudiger HA, Selzner N, Thomas DW, Sindram D, Clavien PA. Transgenic mice overexpressing human Bcl-2 are resistant to hepatic ischemia and reperfusion. *J Hepatol* 2002; **36**: 218.
 22. Man K, Fan ST, Ng IO, Lo CM, Liu CL, Wong J. Prospective evaluation of Pringle maneuver in hepatectomy for liver tumors by a randomized study. *Ann Surg* 1997; **226**: 704.
 23. Qian JM, Zhang H, Wu XF, Li GQ, Chen XP, Wu J. Improvement of recipient survival after small size graft liver transplantation in rats with preischemic manipulation or administering antisense against nuclear factor-kappaB. *Transpl Int* 2007; **20**: 784.
 24. Klintman D, Li X, Santen S, Schramm R, Jeppsson B, Thorlacius H. p38 mitogen-activated protein kinase-dependent chemokine production, leukocyte recruitment, and hepatocellular apoptosis in endotoxemic liver injury. *Ann Surg* 2005; **242**: 830.
 25. Demir S, Inal-Erden M. Pentoxifylline and N-acetylcysteine in hepatic ischemia/reperfusion injury. *Clin Chim Acta* 1998; **275**: 127.
 26. Gannon DE, Varani J, Phan SH, et al. Source of iron in neutrophil-mediated killing of endothelial cells. *Lab Invest* 1987; **57**: 37.
 27. Ambros JT, Herrero-Fresneda I, Borau OG, Boira JM. Ischemic preconditioning in solid organ transplantation: from experimental to clinics. *Transpl Int* 2007; **20**: 219.
 28. Parks DA, Granger DN. Ischemia-reperfusion injury: a radical view. *Hepatology* 1988; **8**: 680.
 29. Zimmerman BJ, Grisham MB, Granger DN. Role of oxidants in ischemia/reperfusion-induced granulocyte infiltration. *Am J Physiol* 1990; **258**: G185.
 30. Hager PW, Collart FR, Huberman E, Mitchell BS. Recombinant human inosine monophosphate dehydrogenase type I and type II proteins. Purification and characterization of inhibitor binding. *Biochem Pharmacol* 1995; **49**: 1323.
 31. Allison AC, Eugui EM. Purine metabolism and immunosuppressive effects of mycophenolate mofetil (MMF). *Clin Transplant* 1996; **10**: 77.
 32. Allison AC, Eugui EM. Mycophenolate mofetil and its mechanisms of action. *Immunopharmacology* 2000; **47**: 85.
 33. Puglisi RN, Strande L, Santos M, Schulte G, Hewitt CW, Whalen TV. Beneficial effects of cyclosporine and rapamycin in small bowel ischemic injury. *J Surg Res* 1996; **65**: 115.
 34. Grisham MB, Hernandez LA, Granger DN. Xanthine oxidase and neutrophil infiltration in intestinal ischemia. *Am J Physiol* 1986; **251**: G567.
 35. Mayumi T, Chan CK, Clemens MG, Bulkley GB. Zonal heterogeneity of hepatic injury following shock/ resuscitation: relationship of xanthine oxidase activity to localization of neutrophil accumulation and central lobular necrosis. *Shock* 1996; **5**: 324.
 36. Menger MD, Vollmar B. Role of microcirculation in transplantation. *Microcirculation* 2000; **7**: 291.
 37. Serafin A, Rosello-Catafau J, Prats N, Xaus C, Gelpi E, Peralta C. Ischemic preconditioning increases the tolerance of Fatty liver to hepatic ischemia-reperfusion injury in the rat. *Am J Pathol* 2002; **161**: 587.
 38. Ikeda F, Terajima H, Shimahara Y, Kondo T, Yamaoka Y. Reduction of hepatic ischemia/reperfusion-induced injury

- by a specific ROCK/Rho kinase inhibitor Y-27632. *J Surg Res* 2003; **109**: 155.
39. Klintman D, Schramm R, Menger MD, Thorlacius H. Leukocyte recruitment in hepatic injury: selectin-mediated leukocyte rolling is a prerequisite for CD18-dependent firm adhesion. *J Hepatol* 2002; **36**: 53.
 40. Carlos TM, Harlan JM. Leukocyte-endothelial adhesion molecules. *Blood* 1994; **84**: 2068.
 41. Dold S, Laschke MW, Lavasani S, Menger MD, Thorlacius H. Cholestatic liver damage is mediated by lymphocyte function antigen-1-dependent recruitment of leukocytes. *Surgery* 2008; **144**: 385.
 42. Rajesh M, Pan H, Mukhopadhyay P, et al. Cannabinoid-2 receptor agonist HU-308 protects against hepatic ischemia/reperfusion injury by attenuating oxidative stress, inflammatory response, and apoptosis. *J Leukoc Biol* 2007; **82**: 1382.
 43. Teoh NC, Ito Y, Field J, et al. Diannexin, a novel annexin V homodimer, provides prolonged protection against hepatic ischemia-reperfusion injury in mice. *Gastroenterology* 2007; **133**: 632.
 44. Hafez T, Moussa M, Nesim I, Baligh N, Davidson B, Abdul-Hadi A. The effect of intraportal prostaglandin E1 on adhesion molecule expression, inflammatory modulator function, and histology in canine hepatic ischemia/reperfusion injury. *J Surg Res* 2007; **138**: 88.
 45. Man K, Ng KT, Lee TK, et al. FTY720 attenuates hepatic ischemia-reperfusion injury in normal and cirrhotic livers. *Am J Transplant* 2005; **5**: 40.
 46. Song J, Zhang YW, Yao AH, et al. Adenoviral cardiotrophin-1 transfer improves survival and early graft function after ischemia and reperfusion in rat small-for-size liver transplantation model. *Transpl Int* 2008; **21**: 372.
 47. Pandolfi A, Di Pietro N, Siroli V, et al. Mechanisms of uremic erythrocyte-induced adhesion of human monocytes to cultured endothelial cells. *J Cell Physiol* 2007; **213**: 699.
 48. Pietersma A, Tilly BC, Gaestel M, et al. p38 mitogen activated protein kinase regulates endothelial VCAM-1 expression at the post-transcriptional level. *Biochem Biophys Res Commun* 1997; **230**: 44.
 49. Tamura DY, Moore EE, Johnson JL, Zallen G, Aiboshi J, Silliman CC. p38 mitogen-activated protein kinase inhibition attenuates intercellular adhesion molecule-1 up-regulation on human pulmonary microvascular endothelial cells. *Surgery* 1998; **124**: 403.
 50. Ha H, Kim MS, Park J, et al. Mycophenolic acid inhibits mesangial cell activation through p38 MAPK inhibition. *Life Sci* 2006; **79**: 1561.
 51. Gu JJ, Gathy K, Santiago L, et al. Induction of apoptosis in IL-3-dependent hematopoietic cell lines by guanine nucleotide depletion. *Blood* 2003; **101**: 4958.